Available online at www.sciencedirect.com
ScienceDirect
Journal of Sound and Vibration 313 (2008) 395–417
JOURNAL OF SOUND AND VIBRATION
www.elsevier.com/locate/jsvi

Autoresonant control strategies of loaded ultrasonic transducer for machining applications

S. Voronina*, V. Babitsky

Wolfson School of Mechanical and Manufacturing Engineering, Loughborough University, Leicestershire LE11 3TU, UK

Received 9 March 2007; received in revised form 28 October 2007; accepted 10 December 2007
Available online 12 February 2008

Abstract

A computer model of a nonlinear ultrasonic vibrating system with the possibility of autoresonant control is presented. The system consists of two modules, the first of which is an electromechanical model of an ultrasonic transducer comprising a piezoelectric transducer and a step concentrator. The second module simulates an influence from the machining process. Calculation of the coefficients of the electromechanical model was based on the parameters of a real ultrasonic transducer and the process of calculation is explained in detail in the paper. The validity of the created model of the ultrasonic vibrating system has been confirmed experimentally. Further, a model of the autoresonant control of this system has been developed. The autoresonant control maintains the resonant regime of oscillation by means of positive feedback, which provides transformation and amplification of the control signal. The model allows the use and comparison of three control strategies. The first one is based on the feedback signal proportional to the displacement of the end of the concentrator (mechanical feedback). The two other types of control are based on the electrical characteristics of the piezoelectric transducer (electrical feedback). One of these strategies uses the current in the piezoceramic rings as the control signal (current feedback). The last control strategy takes into account both the current and the power of the piezoelectric transducer (power feedback). The results of the simulation are presented and discussed.

1. Introduction

Ultrasonically assisted machining is the superimposition of ultrasonic vibration on a conventional machining processes, such as turning, milling, drilling and other machining techniques, when the vibration is applied directly to a cutting tip (not through the abrasive slurry).

Fig. 1 presents the typical set-up for ultrasonically assisted turning. The ultrasonic transducer consists of piezoceramic rings within a package together with a wave-guide (concentrator) and a back section. A cutting tip is fixed in the tool holder installed at the thin end of the concentrator. The transducer is fixed through its developed nodal cross-section at the machine tool vertical slide. The workpiece is clamped by a three-jaw spindle chuck and rotates universally by a lathe drive.

When the high-frequency electric impulses from an electronic amplifier are fed to the input of the piezotransducer it begins vibrating due to the piezoelectric effect. The vibration excites the longitudinal waves

*Corresponding author. Tel.: +44 1509 227566; fax: +44 1509 227502.
E-mail address: s.v.voronina@lboro.ac.uk (S. Voronina).

0022-460X/$ - see front matter © 2007 Elsevier Ltd. All rights reserved.
doi:10.1016/j.jsv.2007.12.014

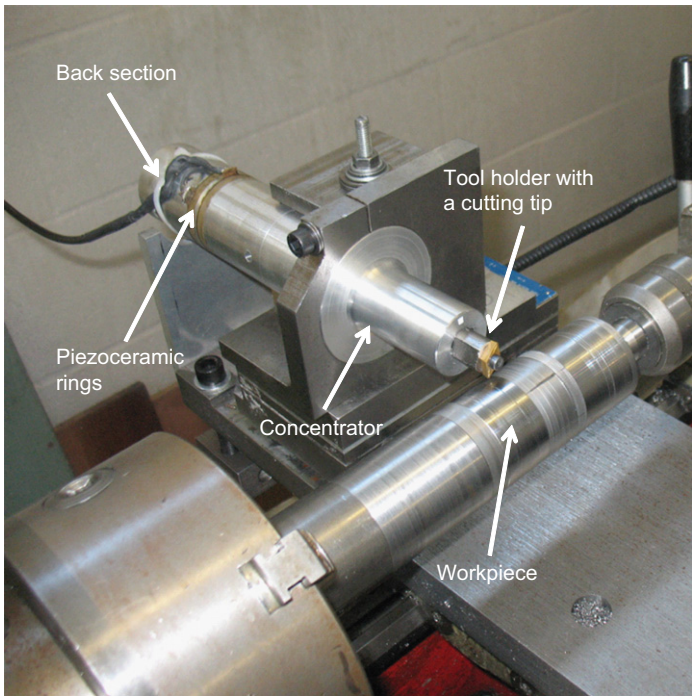

Fig. 1. Experimental set-up of ultrasonically assisted turning.

in the concentrator (which intensifies the amplitude of vibration in the direction of the thin end) and through it the vibration of the cutting tip.

Ultrasonically assisted machining started to develop in the middle of last century (1950s) [1,2]. Since its invention, the method has won recognition and different researchers have reported that, compared to conventional machining technology, it provides a number of benefits, the most important of which are:

- considerable decrease in cutting forces and tool wear;
- improvement of finish quality by up to 50% (surface roughness and roundness);
- processing of a wide range of materials including hard alloys and difficult-to-machine special composites.

Some examples of ultrasonically assisted machining in comparison with conventional machining are presented in Fig. 2. The significant difference in finish quality produced by these techniques can be clearly seen from these pictures. In the case of the ultrasonically assisted drilling of aluminium, the substantial reduction of burr formation is presented. The example of milling glass shows that conventional machining is more likely to produce cracks than the ultrasonically assisted milling which makes a good quality groove.

In spite of all the listed benefits, the ultrasonically assisted machining has still not been properly developed. The key problem in the promotion of ultrasonically assisted machining is development of the proper adaptive control of the ultrasonic vibration. It was shown that frequency control (forced excitation with a prescribed frequency) is inefficient in achieving peak performance of ultrasonic cutting systems [3–5]. The main reasons for this are the nonlinear behaviour of ultrasonic vibrating systems when several regimes are possible with the same frequency applied and the ill-defined nature of the ultrasonic process. The most advanced control method for overcoming these problems is autoresonance [4–6]. Similar control principle called in Ref. [7] as a constant velocity feedback.

Autoresonant control is a self-sustaining excitation of a vibration mode at the natural frequency of a mechanical system, which maintains the resonant condition of oscillation automatically by means of positive feedback based on the transformation (phase shift) and amplification of the signal from a sensor. Depending

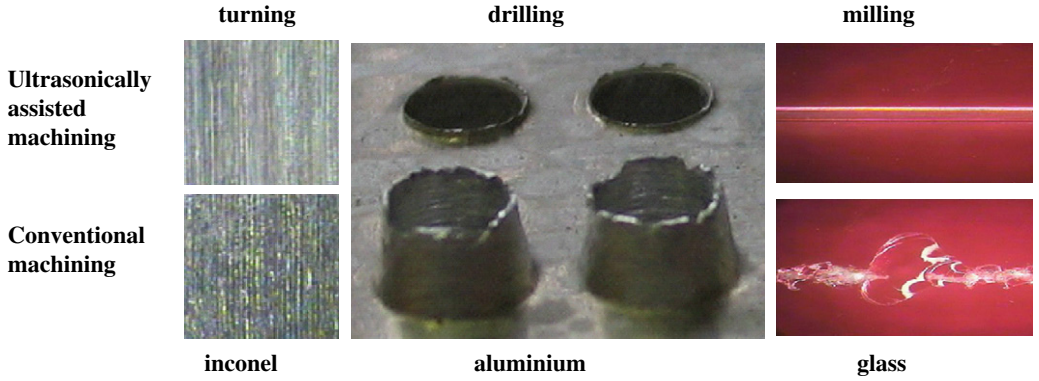

Fig. 2. Comparison of ultrasonically assisted and conventional machining.

on the choice of the sensor, different control strategies can be used, which can be classified into two main types:

- *Mechanical feedback*: When the signal from the displacement (velocity) sensor attached to the end of concentrator or cutting tip is used for the control system.
- *Electrical feedback*: When the signal from the current sensor, measuring the electrical parameters of the piezoelectric transducer (current, power), is used in a control algorithm.

This paper is devoted to the investigation and comparison of control strategies based on mechanical feedback and electrical feedback. The possible benefits and drawbacks of every control strategy will be revealed and considered. The method of investigation is by using numerical simulations, which requires the creation of a model of the ultrasonic vibrating system and a model of the control system.

2. Model of the ultrasonic vibrating system

The model of the ultrasonic vibrating system provides numerous possibilities for the investigation of its properties. However, the ultrasonic transducer is a complex system with many degrees of freedom (DOF) and creating a realistic model is a complicated task. The model is a simplified copy of the original, having the properties of the original system, which are significant for the current application. The results of further investigations will depend on the model and that is why the creation of a reliable model is a very important step. In the literature a large number of papers are dedicated to the modelling of ultrasonic transducers, however the majority of them concentrate on the finite element modelling [8] and very few of them are devoted to the development of one-dimensional numerical computer models accommodating the nonlinear impact interaction as a loading process. One-dimensional numerical models are much faster to process the information required than FE models—i.e. simulations are less demanding on a computer and therefore they appear to be more convenient for evaluation of new control concepts, which can be done easily and quickly. This section is devoted to the modelling of the loaded ultrasonic vibrating system in one dimension and considers the process of system simplification, the development of methods for calculating the model parameters and the nonlinear impact modelling.

Fig. 3 explains the process of simplification that allows the vibrating system to keep the important properties of the original whilst making the model accessible for simulation. Fig. 3(a) represents the ultrasonic transducer consisting of the piezoelectric transducer, concentrator and back section.

Due to the existence of a nodal point between the piezoceramic rings in the working regime of the transducer, the back section of the transducer can be neglected and an ultrasonic transducer can be substituted with the model consisting of one piezoceramic ring and a concentrator (see Fig. 3(b)). The left end of this structure is treated as unmovable.

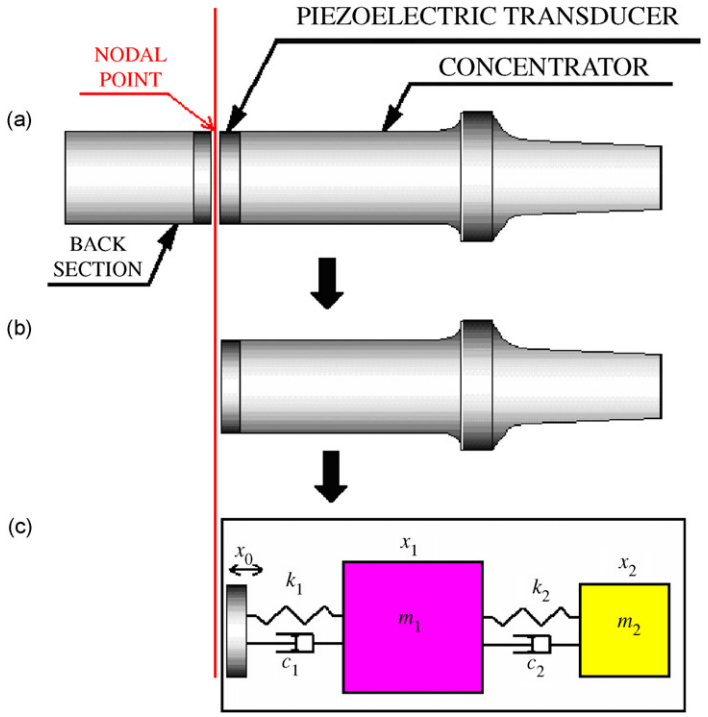

Fig. 3. Two steps simplification for modelling of the transducer.

The strong filtering effect of the concentrator permits considering the model of the concentrator of the ultrasonic transducer as a two-degree-of-freedom (2-DOF) system, where the first and the second modes of vibration of the concentrator correspond to the first and the second modes of vibration of the 2-DOF system.

Thus the ultrasonic transducer can be represented as the simplified model shown in Fig. 3(c). This model consists of two parts:

- Model of piezoelectric transducer.
- Model of concentrator-2-DOF vibrating system.

The next step is the calculation of the model's parameters based on existing information, dimensions, constants and so on, which has to be accomplished for both the model of the concentrator and the model of the piezoelectric transducer.

2.1. Model of concentrator

There are many combinations of parameters of a 2-DOF system, which can be used to create the model of the concentrator. To find the "right" combination of parameters the method of calculation based on eigenvalues, eigenvectors and the energy of the original concentrator was developed. This will be described in further details.

Initially, the eigenvalues of the distributed parameters model of the concentrator will be defined. Fig. 4 depicts the design of the step concentrator used in this work. The concentrator consists of two steps bar with different cross-sectional areas. The coordinate of the connection cross-section of the two steps is x_c; whilst S_1, S_2 are the cross-sectional areas of the corresponding first and second steps; L is the full length of the concentrator. In order to describe the longitudinal vibration within the bar, the cross-sections are assumed to remain flat during the vibration and the particles lying in the cross-sections are assumed to move only in

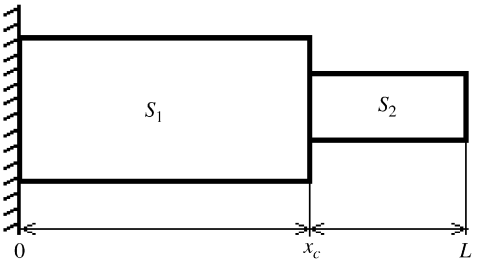

Fig. 4. Step concentrator.

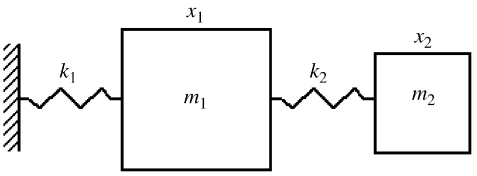

Fig. 5. 2-DOF system, modelling of the concentrator.

the x direction. Let $v(x, t)$ describe the displacement of the cross-section x from its position within the undeformed bar. The equation for the longitudinal vibration within the bar can be written in the form:

$$\mu_i \frac{\partial^2 v_i}{\partial t^2} = S_i E \frac{\partial^2 v_i}{\partial x^2}, \tag{1}$$

where $i = 1, 2$ is the number of the bar considered, $\mu_i = \rho S_i$ is the mass per unit length of the bar, ρ is the bar material density and E is the modulus of elasticity.

Boundary conditions for both the fixed and free ends of the concentrator are written, respectively, as

$$\begin{aligned} v_1(x,t)\big|_{x=0} &= 0, \\ \left.\frac{\partial v_2(x,t)}{\partial x}\right|_{x=L} &= 0, \end{aligned} \tag{2}$$

where $v_1(x, t)$ and $v_2(x, t)$ are the longitudinal displacements within the first and the second steps.

The conditions for the cross-section with coordinate x_c, where two steps join together are as follows:

$$\begin{aligned} v_1(x,t)\big|_{x=x_c} &= v_2(x,t)\big|_{x=x_c}, \\ \left.\frac{\partial v_2(x,t)}{\partial x}\right|_{x=x_c} &= \frac{S_1}{S_2}\left.\frac{\partial v_1(x,t)}{\partial x}\right|_{x=x_c}. \end{aligned} \tag{3}$$

Eq. (1) in relation to Eqs. (2) and (3) describes the distributed parameter model of the concentrator.

Solving Eq. (1) with boundary conditions (2) the modes of oscillation of the first and second steps of the concentrator to be found. Applying conditions (3) to the equations describing the modes of oscillation gives Eq. (4), from which the eigenvalues of the distributed parameters model of the concentrator are obtained as follows:

$$\tan\left(x_c\sqrt{\frac{\rho\omega^2}{E}}\right)\tan\left((x_c - L)\sqrt{\frac{\rho\omega^2}{E}}\right) = -\frac{S_1}{S_2}. \tag{4}$$

It has already been mentioned that the 2-DOF system can be substituted for the distributed parameters model of the concentrator. The parameters of the undamped 2-DOF system (k_1, k_2, m_1, m_2) (Fig. 5) have been chosen to match the eigenvalues, eigenvectors and energy with that of the distributed parameter model of the step concentrator (Fig. 4). Eigenvalues are obtained from Eq. (4), eigenvectors are measured from the

experiment and the full energy of the distributed parameter model is calculated from Eq. (5) and equalised with the full energy of 2-DOF system

$$U = \frac{E}{2}\left[S_1 \int_0^{x_c} \left(\frac{\mathrm{d}v_1}{\mathrm{d}x}\right)^2 \mathrm{d}x + S_2 \int_{x_c}^{L} \left(\frac{\mathrm{d}v_2}{\mathrm{d}x}\right)^2 \mathrm{d}x\right]. \tag{5}$$

Thus the combination of parameters of the 2-DOF system that provides the closest correspondence with the distributed parameter model of concentrator is defined.

2.2. Model of the piezoelectric transducer

The next step is the calculation of the parameters of the model of the piezoelectric transducer. According to the definition, piezoelectricity is a coupling between a mechanical and an electrical behaviour of a medium. That is why the most important function of the model of the piezoelectric transducer is to provide the correlation between the electrical and mechanical parameters of the ultrasonic system. In other words, the model has to define the interaction between the displacement of the piezoelectric transducer, the load from the concentrator and the voltage, supplied to the piezoceramic rings.

To a good approximation, the interaction between the electrical and mechanical qualities of the piezoceramic can be described by linear relations between electrical and mechanical variables:

$$\begin{aligned} \varepsilon &= s^E \sigma + \mathrm{d}\Sigma, \\ \Sigma &= -h\varepsilon + \frac{D}{\xi^s}, \end{aligned} \tag{6}$$

where ε is the strain, σ is the applied stress, s^E is the elastic compliance at constant electric field, d is the piezoelectric charge constant, h is the piezoelectric deformation constant, Σ is the field strength, D is the dielectric displacement and ξ^s is the permittivity at constant strain [9].

Taking into account that

$$\varepsilon = \frac{x_0}{l_0}, \quad \sigma = \frac{F_0}{S_0}, \quad \Sigma = \frac{u}{l_0}, \quad D = \frac{q}{S_0}$$

and rearranging Eqs. (6) transfer to

$$x_0 = \frac{l_0 s^E}{S_0} F_0 + \mathrm{d}u, \tag{7}$$

$$q = \frac{h\varepsilon^s S_0}{l_0} x_0 + \frac{\varepsilon^s S_0}{l_0} u, \tag{8}$$

where S_0 is the area and l_0 is the thickness of a piezoceramic plate, x_0 is the amplitude of deformation for a single piezoceramic plate, F_0 is the force applied to the piezoelectric transducer from the concentrator (will be further considered) and u is the voltage supplied to the piezoceramic plates.

Thus, Eq. (7) describes the state of the piezoelectric transducer and provides the basis for the creation of a model. The model specifies the interaction between the mechanical F_0, x_0 and electrical u parameters of the ultrasonic system. Values l_0, S_0 and s^E will depend on the properties of each particular piezoelectric transducer.

Eq. (8) describes the charge of the piezoelectric transducer. Differentiating the charge with respect to time gives the current of the piezoelectric transducer, which will be further used for the control system based on electrical feedback.

2.3. Model of ultrasonic transducer

Now when the model of the concentrator and the model of the piezoelectric transducer have both been produced a full model of ultrasonic transducer, consisting of the concentrator and the piezoelectric transducer can be derived (Fig. 6).

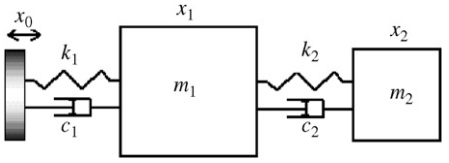

Fig. 6. Model of the ultrasonic transducer.

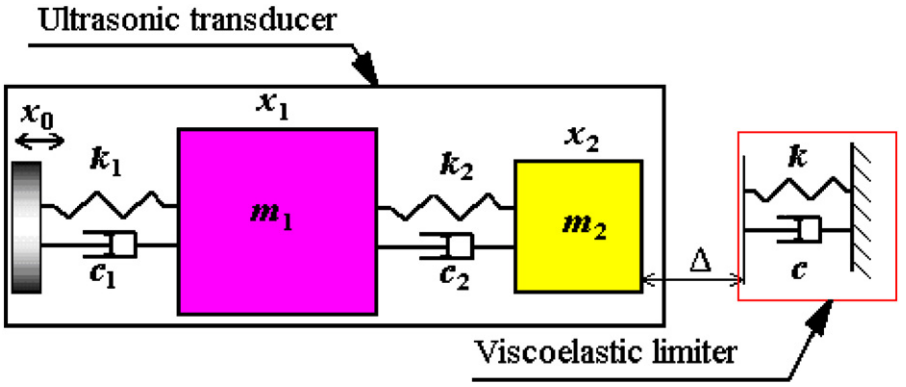

Fig. 7. Model of interaction of the ultrasonic transducer with a load.

Equations of motion for the system, shown in Fig. 6 can be written as

$$\begin{cases} m_1\ddot{x}_1 = -c_1(\dot{x}_1 - \dot{x}_0) - k_1(x_1 - x_0) + c_2(\dot{x}_2 - \dot{x}_1) + k_2(x_2 - x_1), \\ m_2\ddot{x}_2 = -c_2(\dot{x}_2 - \dot{x}_1) - k_2(x_2 - x_1). \end{cases} \tag{9}$$

From here

$$F_0 = c_1(\dot{x}_1 - \dot{x}_0) + k_1(x_1 - x_0) \tag{10}$$

is the force applied to the piezoelectric transducer from the concentrator, and x_0 is the displacement of the piezoelement, described by Eq. (7).

Thus, Eqs. (7), (9) and (10) fully describe the model of the ultrasonic transducer, which has been used for the simulation. The method of calculation of the parameters of the undamped, free, 2-DOF system (k_1, k_2, m_1, m_2) has been described in the previous section. Damping coefficients c_1, c_2 can be selected to provide the amplitudes of oscillation of the first and second bodies just as the amplitudes of vibrations of the first and the second parts of the concentrator, which are obtained experimentally. It is considered here, that the vibration of the first body of the model corresponds to the vibration of the middle of the first step of the concentrator and that the vibration of the second body of the model corresponds to the vibration of the end of the concentrator.

2.4. Nonlinear load design

Application of a load during the process of machining brings strong nonlinearity to the system and instability to the process of control. That is why it is important to simulate the influence from the machining process in the model to investigate the performance of the control system under the load.

One-dimensional contact interaction between the ultrasonic transducer and a workpiece can be described with the help of a viscoelastic limiter, known as a Kelvin–Voigt model (Fig. 7). The limiter is modelled schematically as a parallel working linear spring with stiffness k and a dashpot with damping coefficient c. The initial gap between the ultrasonic transducer and a viscoelastic limiter is defined as Δ; negative Δ corresponds

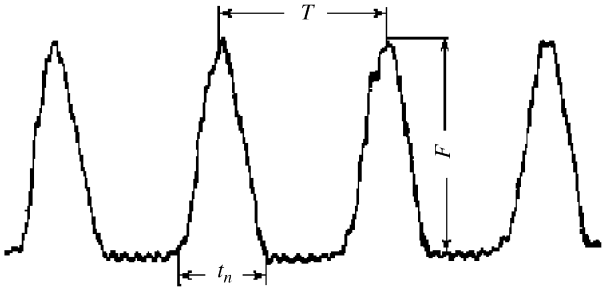

Fig. 8. Oscilloscope reading for the interaction force between the tool and the workpiece. Reproduced from Ref. [10].

to the initial interference. Such a model describes the dynamic loading of the ultrasonic transducer due to processing [3].

The dynamic response of the limiter is described as

$$F = \begin{cases} kx + c\dot{x}, & x > 0, \\ 0, & x \leqslant 0, \end{cases} \tag{11}$$

where $x = x_2 - \Delta$, k is the contact stiffness, c is the contact damping, Δ is the initial interference/gap (Δ will be further used in this paper as the initial interference), x_2 is the displacement of the second body (end of the concentrator).

In order to calculate the parameters of the viscoelastic limiter, the oscilloscope reading showing the interaction force between the tool and a workpiece obtained experimentally is considered (Fig. 8) [10]. It can be seen from the graph that the duration of a contact:

$$t_n \approx 0.5T, \tag{12}$$

where t_n is the time of contact, T is the period of oscillations.

Both initial interference Δ and contact stiffness k exert an influence on the interaction force and impact duration correspondingly. This means that the values of the parameters Δ and k providing the impact duration (12) can be taken for the model. The magnitude of Δ can be chosen as any sufficiently small value, as in practice initial interference depends on the workpiece material and machining conditions. When the value of the initial interference has been chosen, the value of the contact stiffness can be found to comply with the condition (12). The contact damping coefficient for the viscoelastic limiter can be selected so as to make the amplitude of oscillation of the second body of the model the same as the amplitude of oscillation of the end of the concentrator during the process of dynamic loading as obtained experimentally.

Fig. 9 shows simulation results for the model of the ultrasonic transducer with the load applied. A comparison of the graph for the interaction force obtained as a result of the simulation (Fig. 9(b)), with the interaction force obtained as a result of experiment (Fig. 8), shows their agreement. This proves the validity of the created model of the contact interaction.

2.5. Matlab–Simulink model

Finally, the models of all parts of the ultrasonic vibrating system and the model representing the influence of the machining process have been developed. Based on the described formulae, Eqs. (7), (9), (10) and (11), the parameters of these models have been calculated and the Matlab–Simulink model of the system described above was created. A general schematic of this model is presented in Fig. 10.

The model provides several regimes of oscillations:

- *Forced oscillations*: Open-loop oscillation using the sine wave with prescribed frequency and amplitude of oscillation as a voltage signal for the piezoceramic transducer (Fig. 10, switch 1).
- *Autoresonant control*: Closed-loop oscillation with a positive feedback, providing phase shifting and amplification of a signal from a sensor. The control strategies of two main types (mechanical feedback and

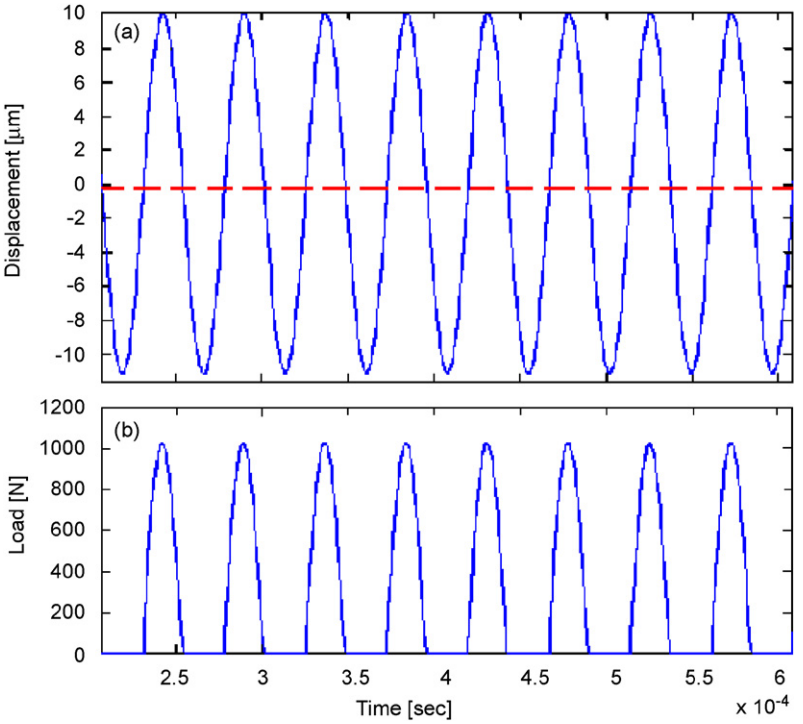

Fig. 9. Simulation of ultrasonic transducer with the load applied: (a) solid curve is the displacement of the second body x_2; the dashed line is the interference value Δ, and (b) load applied.

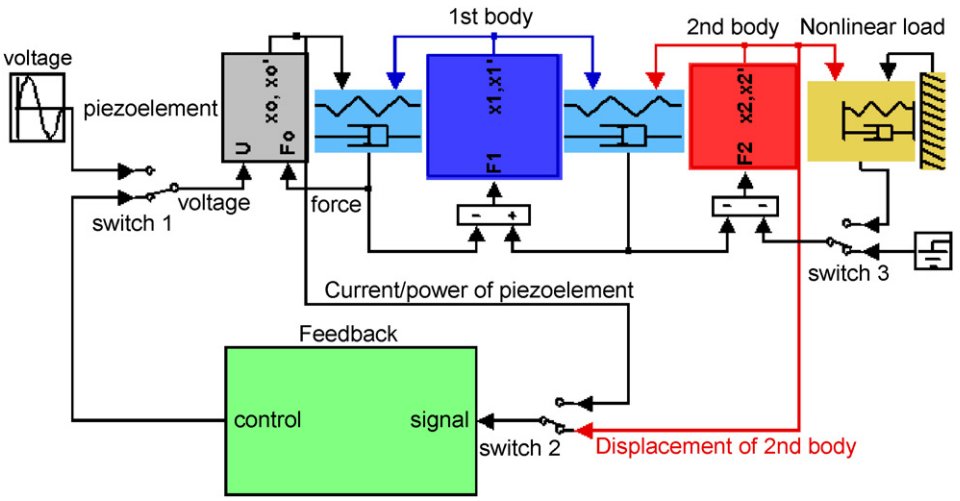

Fig. 10. Matlab–Simulink model of the ultrasonic vibrating system with a nonlinear load and a possibility of the autoresonant control.

electrical feedback) have been implemented (Fig. 10, switch 2). The design of the model of the control system will be considered in the next section.

- *Loaded oscillations*: Both described above regimes can be used with or without a nonlinear load applied (Fig. 10, switch 3).

Thus development of the model of the ultrasonic vibrating system has been completed. Verification of the created Matlab–Simulink model will be considered in the next section. The next step is to develop the model of the control system.

3. Model of the control system

The created model of the ultrasonic vibrating system allows the simulation of operation of the ultrasonic transducer under different cutting conditions. In order to make possible the investigation of different control strategies, the model of the control system based on the principle of autoresonance [5] has to be developed. The process of developing the model of the control system, including the theoretical investigation of different control strategies, will be discussed within this section.

3.1. The principle of autoresonance control

Autoresonant control is a method based on phase control [11], which maintains the resonant regime of oscillation automatically by means of positive feedback using transformation (phase shift) and amplification of the signal from a sensor. It is based on the fact that during resonance the phase lag between the vibration of the working element (cutter) and the excitation force applied to the latter is constant. A general schematic of feedback is presented in Fig. 11.

3.2. Control system algorithm

The main purpose of the control system is to keep the vibrations of the ultrasonic transducer at a specified level during the process of cutting (the regime of oscillations with the nonlinear load applied). The description of the control system operation is provided below.

The control system generates a control signal by means of shifting the phase of the signal from the sensor and changing its amplitude. This control signal is then supplied to the piezoelectric actuator to produce an excitation for the vibrating system. To perform this algorithm initially, the phase shift giving the maximum amplitude of vibration needs to be found and set up. Thus the most efficient autoresonant state of the system is reached. It is known that the application of the nonlinear load changes the resonant frequency of the system [5] and affects the level of vibration. To keep the resonant mode of oscillations, the phase shift value has to be changed along with the alteration of the nonlinear load. This is accomplished by the following phase control algorithm.

For every control cycle the phase shift value is changing by the phase control unit value and the RMS value of the sensor signal is traced. If the RMS value of the sensor signal obtained from the next control cycle after changing the phase shift is less than the RMS value of the sensor signal obtained from the previous control cycle (when the phase shift was changed), the direction of changes of phase shift is changed to the opposite one. Otherwise the direction of changes is kept the same. Thus the control system always aims at the most efficient autoresonant state.

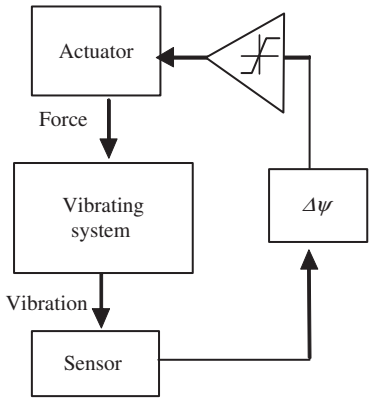

Fig. 11. General schematic of feedback.

To compensate for the losses in amplitude occurring due to loading, amplitude control is used. Amplitude control is designed to keep the amplitude of oscillations during cutting at the level prescribed by the programme. To provide this control, the system is constantly observing the amplitude of the sensor signal (the RMS value is used as a measure). When this value enters the critical zone (i.e. changes by more than 5% of desired value), the control system calculates the new value for the amplitude of the control signal according to the specific algorithm. Setting this value up allows the desired level of oscillations to be approached.

Thus, the combined amplitude–phase control algorithm allows the possibility of simultaneous control of the resonant state (phase control) and level of oscillations (amplitude control), which ensures stable oscillations at the most efficient resonant mode.

3.3. Mechanical feedback and electrical feedback

Depending on choice of the sensor, two different control strategies are possible:

- Mechanical feedback when the sensor, measuring the mechanical characteristics of the oscillations (displacement, velocity or acceleration) attached to the end of the concentrator is used for the control system.
- Electrical feedback which uses the signal from any electrical sensor measuring the electrical characteristics of the piezoelectric transducer (current, voltage, or power).

Let us now consider the advantages and disadvantages of these control strategies. Mechanical feedback uses a sensor measuring vibration (it could be a displacement, velocity or acceleration sensor). The sensor is placed near the cutting area at the end of the concentrator or at the cutting tip. Therefore, it directly reflects the oscillations of the ultrasonic system and, by controlling the signal from this sensor, the actual state of vibration can be controlled in the most efficient way. However, it is inconvenient to use this arrangement in industrial conditions, since it is difficult to fix the sensor permanently because of prolonged high-frequency vibration under harsh machining conditions. Additional wiring to the control system is a disadvantage as well, as the sensor is located in the cutting area.

Electrical feedback uses the electrical characteristics of the piezoelectric transducer for the control, i.e. current or power. An electrical sensor does not need to be placed in the cutting area, which makes it convenient to use in industrial conditions. However, this sensor reflects the oscillations of the system in an indirect way via the current or power in the piezoceramic rings. This can cause difficulties for the control system, which will be further discussed.

3.3.1. Theoretical investigation of feedback types

A simplified model of an ultrasonic transducer representing the 2-DOF system is shown in Fig. 6. It is known that the 2-DOF system has different amplitude–frequency–phase curves, depending on the choice of points used to define the phase shift between the vibration and force application point [11]. In the case of the described model of the ultrasonic transducer, the excitation force is applied to the first body, but there are two different observation points of phase shift definition:

- In the case of mechanical feedback, the sensor is attached to the end of the concentrator, which means that the point of observation is the second body.
- In the case of electrical feedback, an electrical characteristic of the piezoelectric transducer is used as the control signal. The current of the piezoelectric transducer according to Eqs. (7)–(10) mainly reflects the vibrations of the first body, i.e. the point of observation is the first body.

To investigate the main properties of the model of an ultrasonic transducer under phase control, the analytical solution of the equations of motion has been completed and the amplitude–phase curves for both described cases have been obtained (Fig. 12). The amplitude–phase characteristic of the first body of the model of ultrasonic transducer is shown in Fig. 12 as the dotted curve; the amplitude–phase characteristic of the second body of the model is shown as the solid curve.

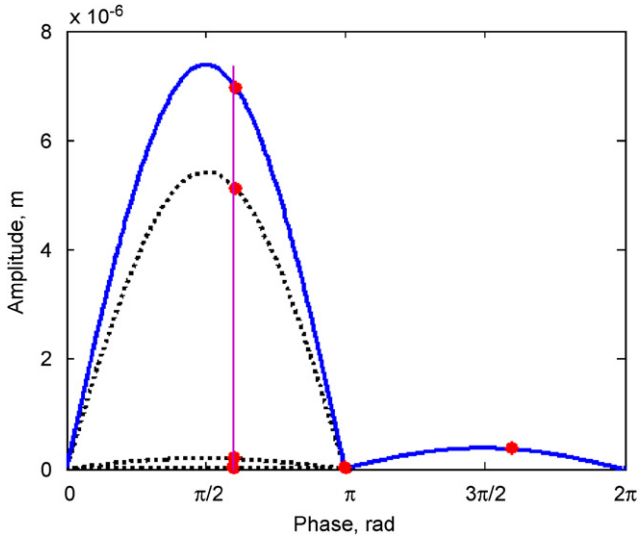

Fig. 12. Amplitude–phase characteristics of the model of ultrasonic transducer for two feedback types: the point of observation is the first body—dotted line and second body—solid line.

The following qualities can be seen from this figure:

- the amplitude–phase curves of the system are bell-shaped and smooth near the resonance, which proves the fact that using the phase control the resonant mode of oscillation can be easily controlled;
- the amplitude–phase characteristic of the first body is ambiguous, whereas the amplitude–phase curve of the second body is single valued.

The latter result means that three vibration states are possible in the system under phase control for any phase shift near the resonant $\pi/2$ value when the same body is used both for excitation and observation. The corresponding points of the curves are marked with the bold dots. Two of these states are resonant regimes for the first and second oscillation modes correspondingly, and the third state with the lowest amplitude corresponds to anti-resonant vibration. Investigation of the stability of these states has shown that the both resonant states are stable. Hence, two stable regimes with different amplitudes and frequencies can exist for the same phase in the considered model under phase control, when the first body is chosen to observe an oscillation and to apply excitation. This result means that two regimes can be excited in the system (either the first resonant regime or the second one) under phase control, when the signal from the current sensor is used as a control signal. This advises introducing a filtration procedure into electrical feedback control to make sure that the "right" resonant regime (the regime with the specified frequency) is excited.

Using the filter for the autoresonant closed-loop system brings considerable difficulties into the control algorithm, because the filter shifts the phase of the incoming signal and changes its amplitude in the band pass. The effectiveness of electrical feedback control including a filter will be further considered.

3.3.2. Amplitude–frequency characteristics of electrical signals in comparison with the amplitude–frequency characteristic of displacement signal

It was mentioned above that electrical sensors reflect the oscillations of the ultrasonic system in an indirect way via the current or power of piezoceramic rings. In order to check the impact it makes on the control system, an investigation to compare the electrical signals (current and power) with the displacement signal has been completed. The experimental investigation included obtaining and comparing the amplitude–frequency characteristic for the displacement of the end of the concentrator with the amplitude–frequency characteristics for the current and power of the piezoelectric transducer.

During the experiment, a swept sine wave was used to slowly sweep the dynamic system through a range of excitation frequencies. The signals from the sensors together with the generated sweep sine wave were captured using a digital data-recording oscilloscope and transferred to a personal computer for subsequent processing. The average power of the piezoelectric transducer was calculated in Matlab–Simulink according to the following formula:

$$P = \frac{1}{T}\int_0^T iu\,\mathrm{d}t, \tag{13}$$

where i is the current and u is the voltage of the piezoceramic transducer as recorded during the experiment; T is the calculated period of the oscillations.

The results of this experiment are shown in Fig. 13. It can be seen from the graph that the resonant peak of the displacement curve (a) coincides very well with the peak of the power curve (b), but does not agree with the peak of the current curve (c). As was explained above, the control signal algorithm always aims at the regime with the maximum amplitude of the sensor signal. This means that, according to experiment, using the signal from current sensor in the control algorithm does not permit the maximum vibrations to be reached.

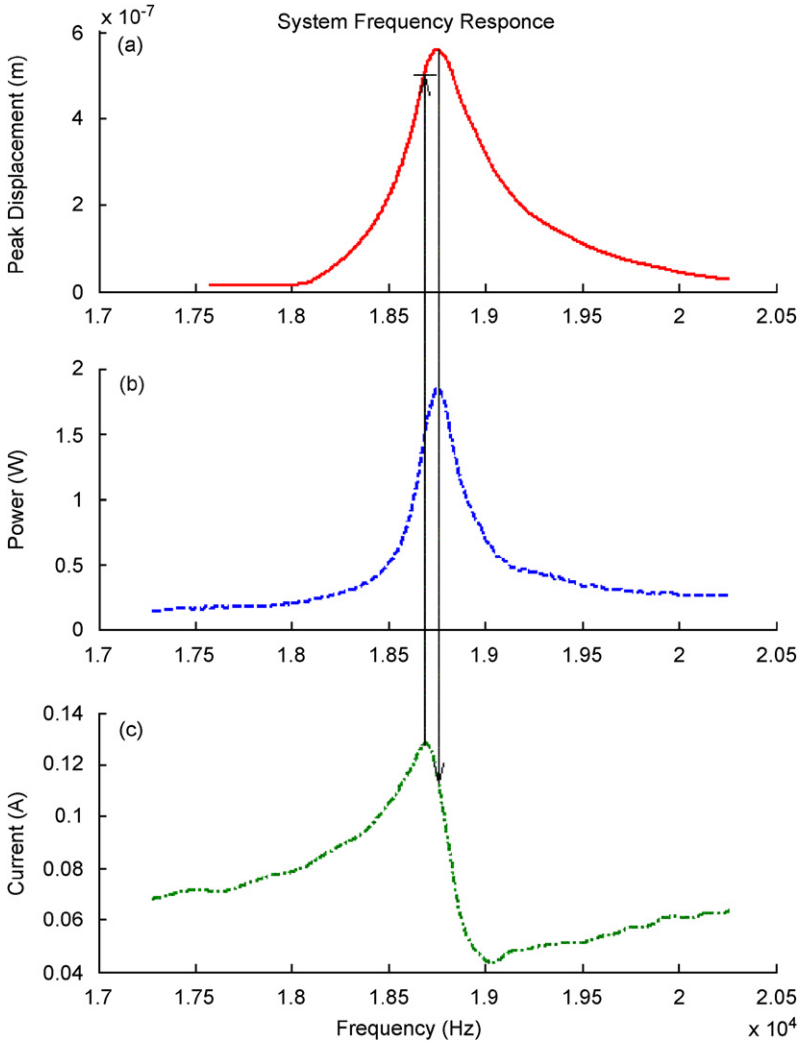

Fig. 13. Amplitude–frequency characteristics. Experimental results: (a) displacement of concentrator's end; (b) power of piezoelectric transducer; and (c) current of piezoelectric transducer.

The amplitude of the displacement signal, which can be obtained using current control, differs by 12.5% from the maximum amplitude of displacement. It was suggested that the difference in amplitude could be compensated for by the initial increase in the amplitude of the voltage supplied to the piezoelectric transducer. This suggestion will be further investigated. For the case of power control, it is possible to reach the maximum amplitude of displacement as the resonant frequencies of power and displacement coincide. This finding will be further investigated in the next section.

In order to verify the created model of the ultrasonic transducer, the same test was repeated for the model. In this case the amplitude–frequency curves of displacement of the second body's current and power were obtained. The results of the simulations are presented in Fig. 14. Comparison of the results of the experiment (Fig. 13), with the result of the simulation (Fig. 14) shows that the simulation curves conform to the experimental curves: i.e. the shapes of the simulation curves are very similar to the experimental ones. The next observation is the coincidence between the resonant frequencies of displacement and power and the lack of coincidence between the resonant frequencies of displacement and current. Good agreement of the experimental and simulation results proves the validity of the model.

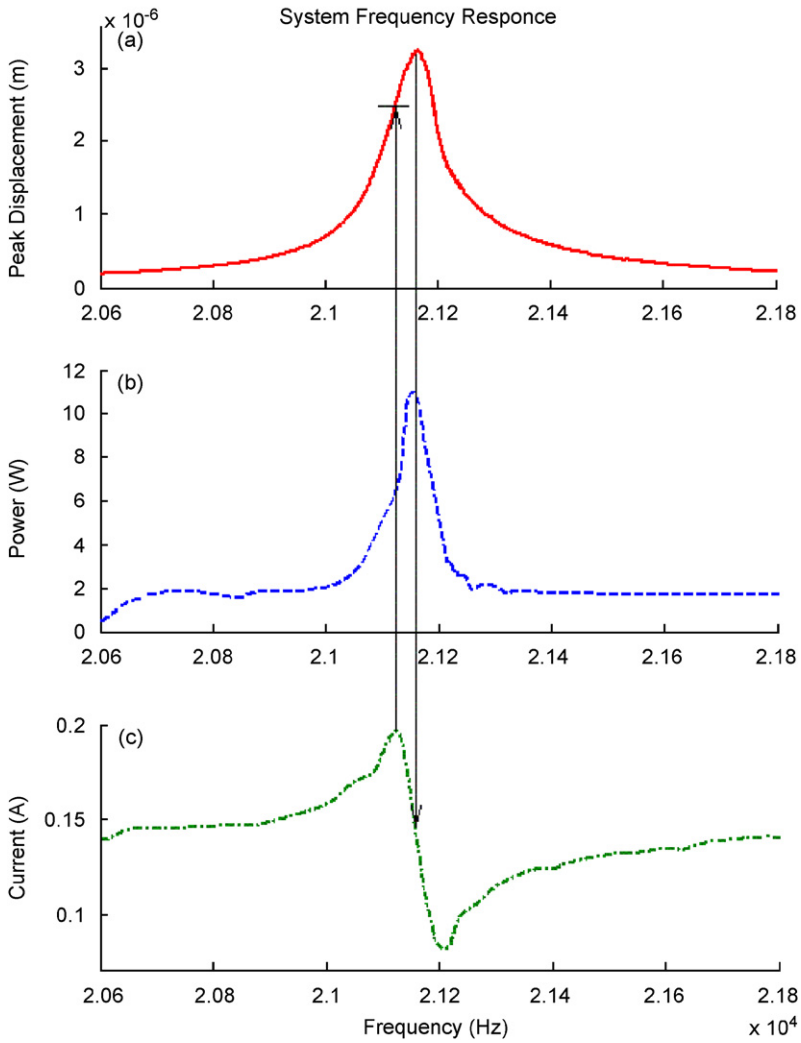

Fig. 14. Amplitude–frequency characteristics. Simulation results: (a) displacement of second body; (b) power of piezoelectric transducer; and (c) current of piezoelectric transducer.

4. Numerical simulations and discussion

The previous section was devoted to the development of the control algorithm and the investigation of the properties of the control strategies based on mechanical and electrical feedbacks. Theoretical investigation showed that electrical feedback requires a more sophisticated control algorithm. In this case, the filtration procedure has to be included in the control algorithm, which can cause additional difficulties for the autoresonant closed-loop system, as the filter changes the phase shift in the feedback loop. Experimental investigation demonstrated the potential inefficiency of an electrical feedback control system using the current signal, due to the shift in the resonant frequencies of displacement and current. The second important observation following from this experiment is the coincidence of the resonant frequencies of the displacement and power signals, which promotes the idea of using both current and power signals for the control system.

Based on the results set out in the previous section, the following control strategies have been further investigated:

1. Mechanical feedback, when the displacement signal was used in the control algorithm (*displacement feedback*).
2. Electrical feedback, when the current signal was used for the control system. This strategy will be called *current feedback*.
3. Electrical feedback, when a current signal was used as the control signal to generate excitation for the piezoelectric transducer and a power signal was used to define the actual performance of the system. This control strategy will be further called *power feedback* control.

Now the results of the control system simulation for three described types of control will be presented and discussed. In order to investigate the ability of the control system to keep the desired level of vibrations during the cutting process, the simulation of changes in the loading conditions was carried out.

During the simulation, the load applied to the end of concentrator was changed and the RMS value of the sensor signal was recorded. Two types of tests were conducted: increasing the load applied to the concentrator by changing the contact stiffness value and by changing the interference value.

4.1. Mechanical feedback (displacement control)

Simulation results for the case of mechanical feedback will be now considered. The first test (Fig. 15) investigates the ability of the displacement control to keep the level of vibrations under control in conditions of contact stiffness changing. For illustrative purposes the contact stiffness value (Fig. 15(c)), and the load applied to the ultrasonic system (b) were monitored together with the displacement of the second body (a). The control system uses the RMS value of the displacement signal as a control signal, which is shown in Fig. 16 as a solid line, the dashed line depicts the desired value of the RMS of the displacement signal. The desired value was defined as the RMS of the desired value of the amplitude of displacement of the loaded system.

Fig. 15 shows that with an increase of the contact stiffness value (c) the amount of load (b) was increasing as well. However, in spite of considerable changes of nonlinear load, the amplitude of the displacement was kept stable. Fig. 16 is consistent with Fig. 15 and shows that the RMS value of the displacement was kept close to the desired level during the whole process of simulation. Another interesting observation from Fig. 15(a) is the "shifting" downward of the displacement with the increase of the contact stiffness value, which makes the displacement curve less symmetrical. This illustrates that the increasing contact stiffness makes it more difficult for the ultrasonic transducer to penetrate into the material. That leads to quasi-static compression of the system.

The next test shows the influence of changes in the interference value (and load correspondingly) on the control system performance. Fig. 17(b) depicts the applied load value, which is changing with the increase of the interference value. The effect of the "shifting" downward of the displacement value is also presented Fig. 17(a).

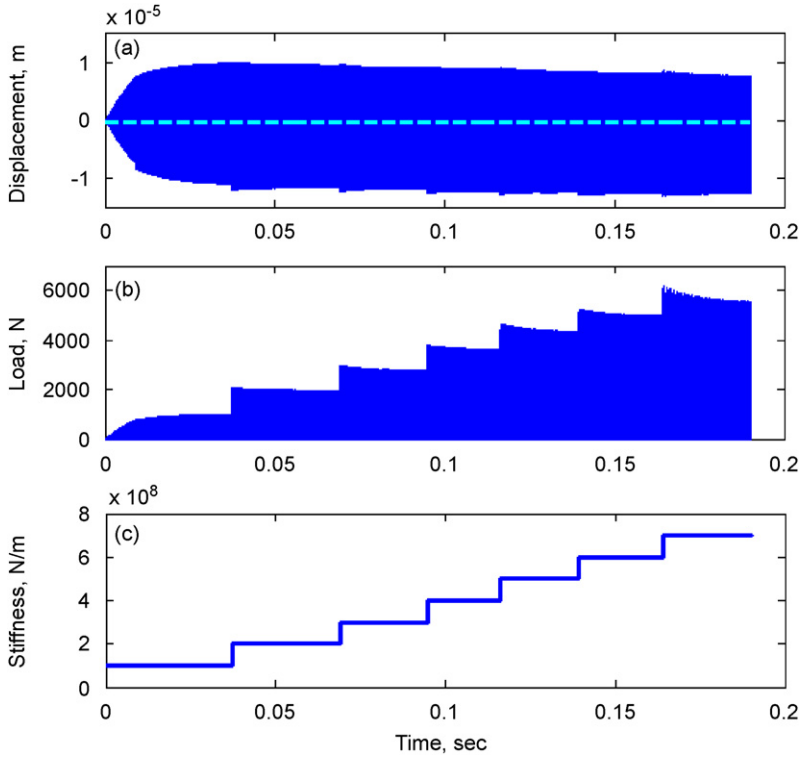

Fig. 15. Mechanical feedback control during changing the contact stiffness: (a) displacement of end of the concentrator; (b) load applied; and (c) contact stiffness value.

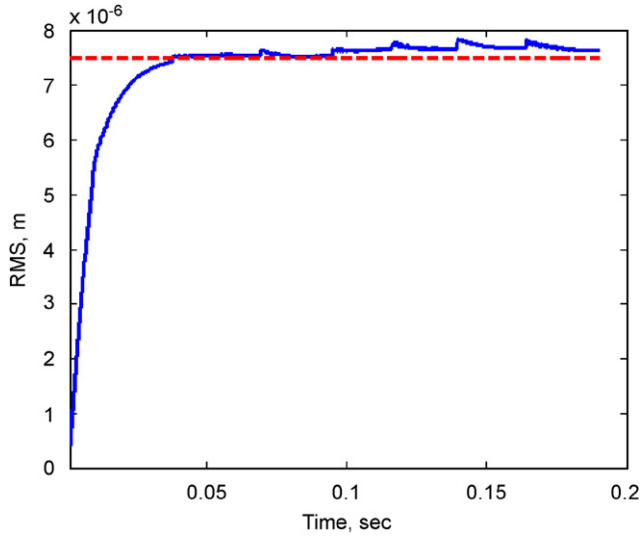

Fig. 16. The RMS value of displacement signal—solid line and desired value of RMS—dashed line.

Again we can see from Fig. 18 that the control system keeps the RMS value quite stable in spite of a considerable increase in loadings.

The results of the both tests have proved that an autoresonant control system based on mechanical feedback is able to maintain the level of vibrations during the process of cutting (in the conditions of the nonlinear load changing).

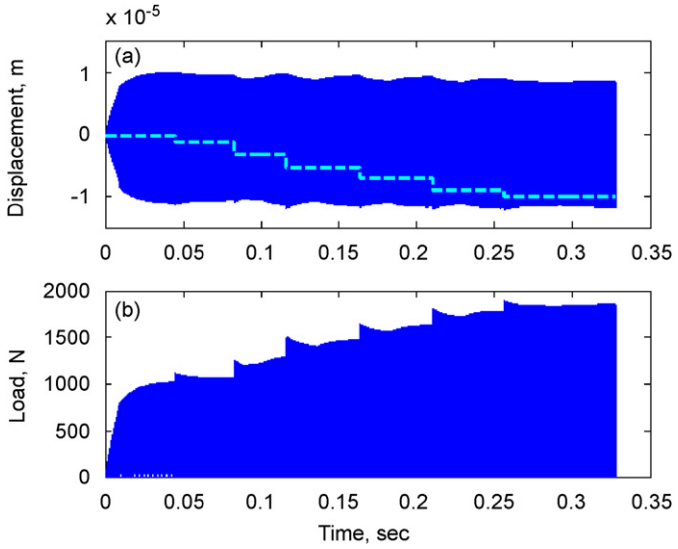

Fig. 17. Mechanical feedback control during changing the interference: (a) displacement of end of the concentrator and interference value (light line) and (b) load applied.

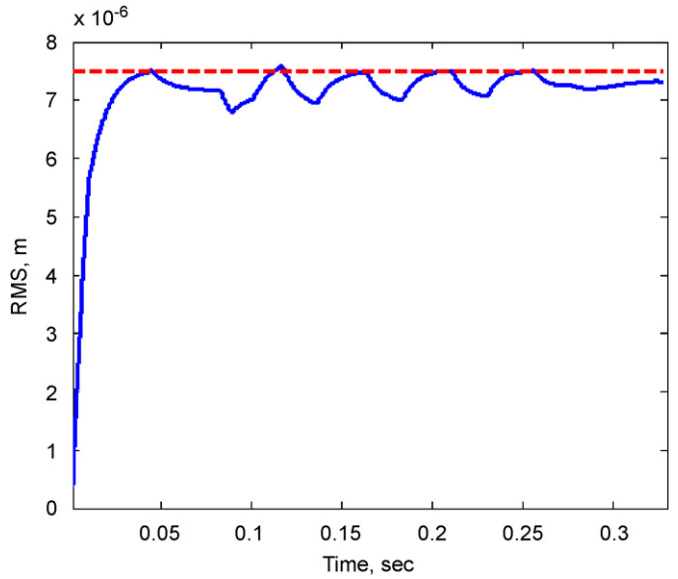

Fig. 18. The RMS value of displacement signal—solid line and desired value of RMS—dashed line.

4.2. Electrical feedback

4.2.1. Current control

In order to compare different control strategies, the simulation of changing the contact stiffness value was repeated for the electrical feedback case. Current feedback when the RMS value of the current of the piezoceramic rings was used as a control signal will be considered first (see Fig. 19).

From the investigation of amplitude–frequency characteristics (see previous section), we know that when using the current signal for the control system, a displacement with amplitude 12.5% less than maximum (desired value) can only be reached. That is why the initial amplitude of the voltage will be increased for this test to compensate for the 12.5% difference and allow the desired value of the displacement to be reached the

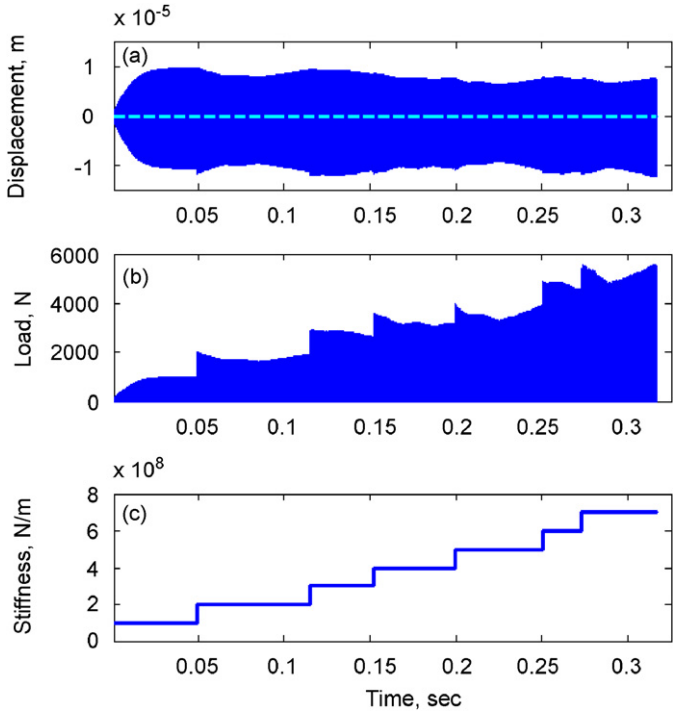

Fig. 19. Current feedback control during changing the contact stiffness: (a) displacement of end of the concentrator; (b) load applied; and (c) contact stiffness value.

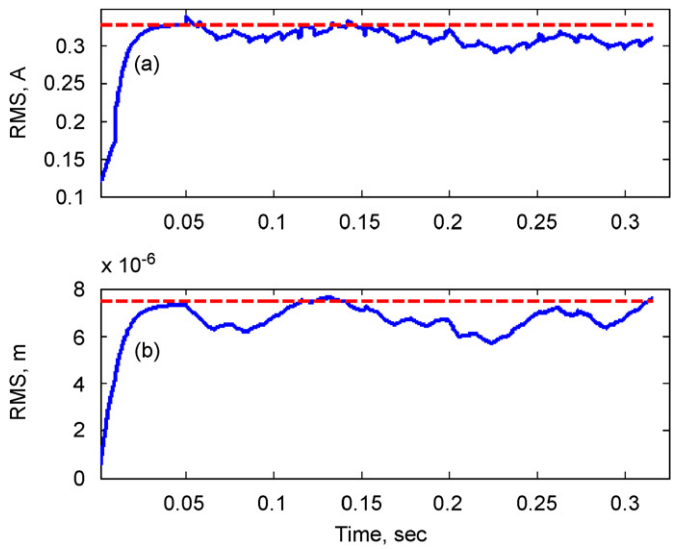

Fig. 20. (a) The RMS value of current—solid line, desired value of RMS—dashed line and (b) RMS value of displacement signal—solid line, desired value of RMS—dashed line.

same, as in previous simulation. To define the required increase, the voltage amplitude was gradually increasing until the RMS of displacement reached its desired value. Thus, the desired value of the current and the initial amplitude of the voltage for the electrical feedback simulation were defined.

In this test, in order to have a clear representation of what is happening with the oscillations of the system, the RMS value of the displacement (Fig. 20(b)) was observed together with the RMS value

of the current (Fig. 20(a)). From these figures we can see that the control system maintains the RMS value of the current (Fig. 20(a)). However, the RMS value of the displacement (Fig. 20(b)) and amplitude of vibrations (Fig. 19(a)), deviates considerably from its desired value during the test. The maximum deflection of the RMS value of the displacement from the desired value is 1.8 μm (24%), which is noticeably higher than the maximum deflection for the displacement control (0.4 μm (5%) from Fig. 16). This test shows that an autoresonant control system based on current feedback was unable to control the level of vibrations during this test.

From a comparison of the two tests, we can see that current feedback is much less suitable for control than displacement feedback. This can be explained due to the shift of the resonant frequency of the current from the resonant frequency of the displacement. Even increasing the voltage supplied to the piezoelectric transducer,

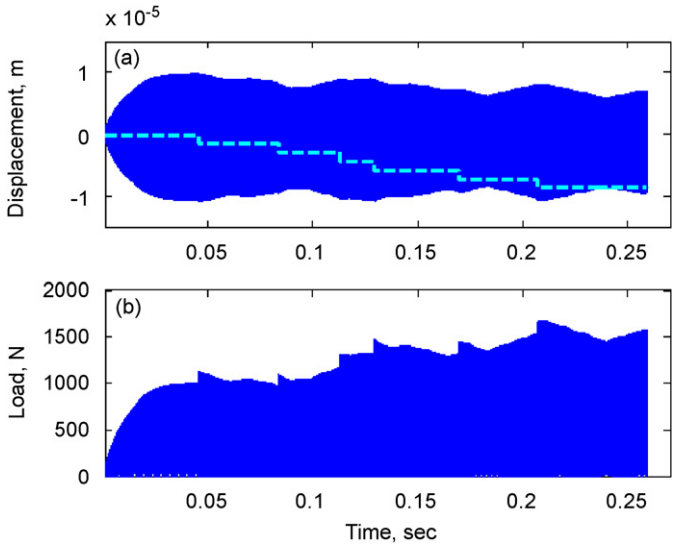

Fig. 21. Current feedback control during changing the interference: (a) displacement of end of the concentrator and interference value (dashed line) and (b) load applied.

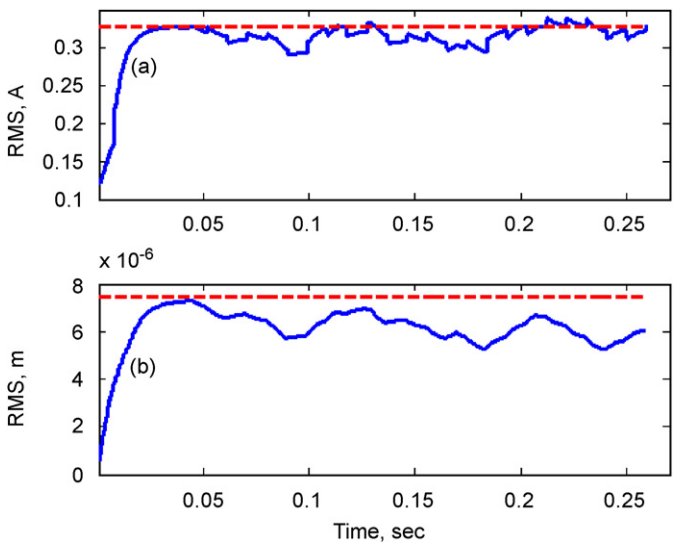

Fig. 22. (a) The RMS value of current—solid line, desired value of RMS—dashed line and (b) RMS value of displacement signal—solid line, desired value of RMS—dashed line.

which was undertaken to compensate for the difference in amplitude, did not solve this problem. Because of the difference in amplitude–frequency curves, controlling the level of current we cannot control the level of displacement properly. This difference can further increase with changes of the load.

The next test shows the influence of changes in the interference value (and load correspondingly) on the control system performance for the current feedback case. Fig. 21(a) depicts the displacement of the second

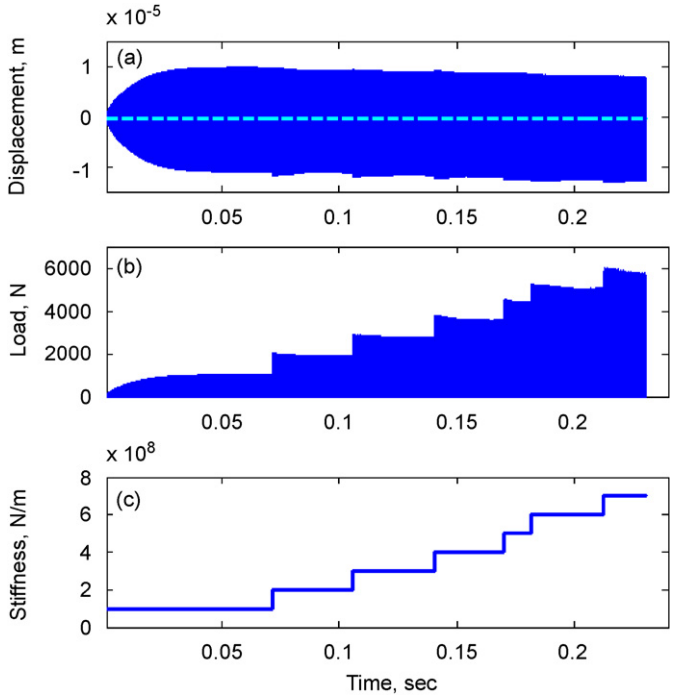

Fig. 23. Power feedback control during changing the contact stiffness: (a) displacement of end of the concentrator; (b) load applied; and (c) contact stiffness value.

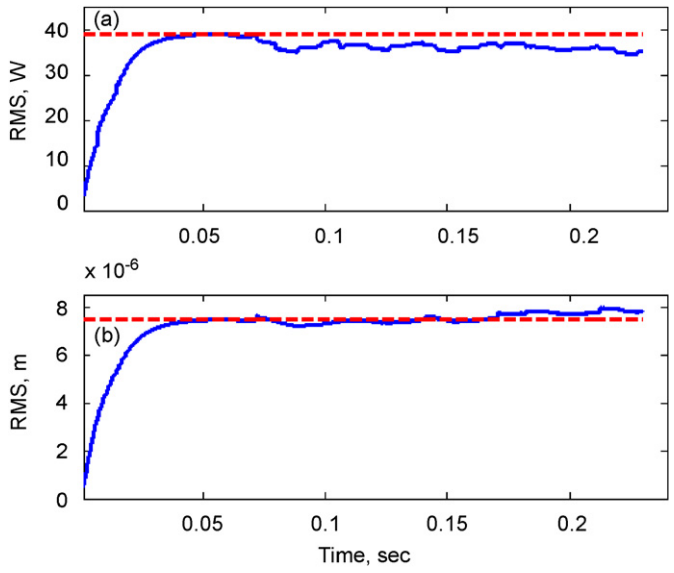

Fig. 24. (a) The RMS value of power—solid line, desired value of RMS—dashed line and (b) RMS value of displacement signal—solid line, desired value of RMS—dashed line.

body and the interference value (light dashed line), which was changing during this test, Fig. 21(b) shows the applied load.

Fig. 22 shows the RMS value of the current signal (a) and the RMS value of the displacement of end of the concentrator (b). We can see that the RMS value of current was kept quite close to the desired value during the whole test, while the displacement was deviating from its desired value. The maximum deflection of the RMS value of the displacement from the desired value is 2.3 μm (30%), which is noticeably higher than the maximum deflection for the displacement control 0.7 μm (9%) from Fig. 18. Results of this test are consistent with the results of previous test and prove inefficiency of the control system based on the current feedback.

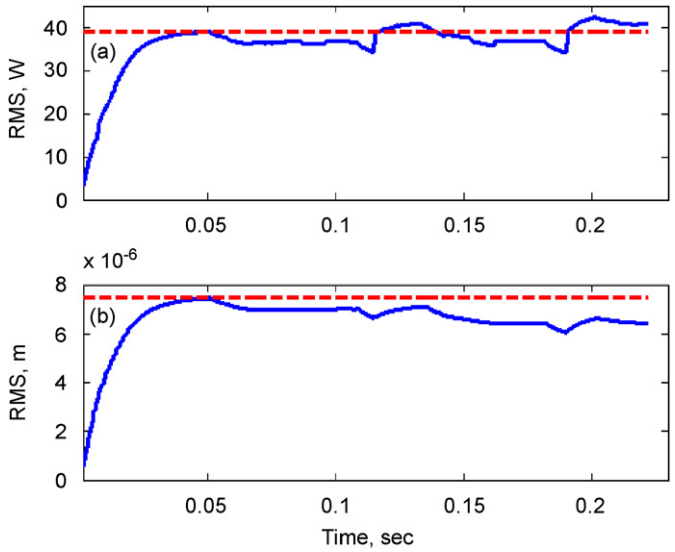

Fig. 25. Simulation of the change of interference: (a) RMS value of power—solid line, desired value of RMS—dashed line and (b) RMS value of displacement signal—solid line, desired value of RMS—dashed line.

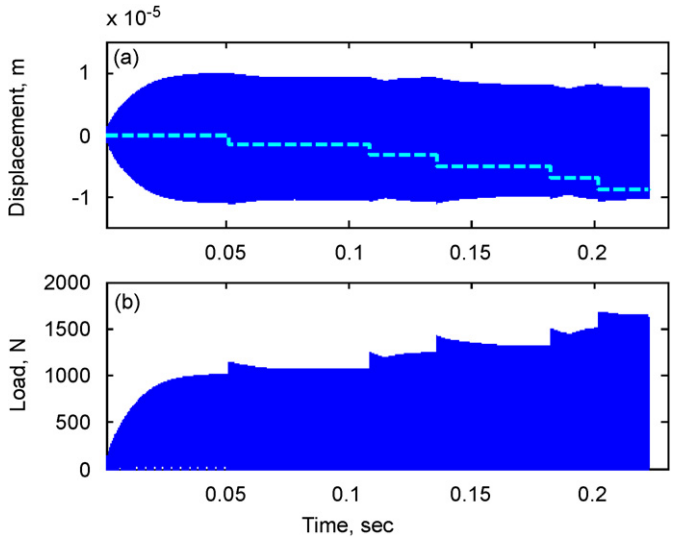

Fig. 26. Power feedback control during changing the interference value: (a) displacement of end of the concentrator and interference value (light line) and (b) load applied.

4.2.2. Power control

Simulation results for the next case of electrical feedback when both the current and the power of the piezoelectric transducer are used in the control algorithm will be now considered. In this case the control system uses the current signal to generate excitation for the vibrating system by phase shifting and amplifying it, as in the case of current control. However, in order to define the required amount of phase shift and amplitude, the control system uses the power signal. From an investigation of amplitude–frequency characteristics we know that the resonant frequencies of the power of the piezoelectric transducer and the displacement of the end of the concentrator coincide. Based on this fact, we make a suggestion that changes in displacement can be better traced using the power signal than by using the current signal, and that, by maintaining the level of power we can keep the level of displacement. This hypothesis will now be investigated. The same test on changing the contact stiffness value for the power feedback case will be considered now (Fig. 23).

The RMS value of the power is presented in Fig. 24(a). To trace the vibrations of the system, the RMS value of the displacement was observed (Fig. 24(b)). From this graph we can see that indeed the power control is able to keep the level of vibrations at the desired value. The maximum deflection of the RMS value of displacement from the desired value is 0.5 μm (7%), which is much better than for the current feedback control (24%) and very close to the result of the mechanical feedback case (5%). This simulation shows that using the power signal for the control system considerably improves the results of electrical feedback control.

However, the following problem occurs with power feedback: any increase in the amplitude of the voltage supplied to the piezoelectric transducer also causes an increase in power. The formula for calculating the power consists of two components: the current and the voltage of the piezoelectric transducer (see Eq. (13)) and increasing one of the components will also increase the power. At the start of the test the desired value of power is defined for the initial level of voltage. Every time when the amplitude control is applied the amplitude of the voltage supplied to the piezoelectric transducer is increased, which increases the level of power, however, the desired value of power is kept the same. This means that the value of the power initially corresponding to the desired level of vibrations will, after an increase in amplitude, correspond to a lower level of vibrations. By maintaining the level of power we cannot control the level of vibrations.

This can be seen from Fig. 25, which depicts the results of the test on changing the interference value for the power feedback case. One can see that, at the beginning of simulation, the desired value of power corresponds to the desired value of displacement. With a change of interference (Fig. 26), the desired value of power corresponds to the desired value of displacement less and less. From this graph we can see that the power control is not as efficient as in the previous test (Fig. 24). In this case, the maximum deflection of the RMS value of displacement from the desired value is 1.4 μm (19%), while for the test on contact stiffness changing it was only 7%.

To avoid this problem the desired value of power has to be increased together with increasing the amplitude of voltage supplied to the piezoelectric transducer. However, it is difficult to identify the increase in the desired value required to compensate for the increase in the amplitude of the supplied voltage, because there is no linear dependence between these characteristics.

Comparing the results of this test with the results of the same test for other feedback types, we can see that the maximum deflection for the power control (19%) is far from the displacement control (9%), but still better than for the current control (30%).

This means that the characteristic of power feedback described above does not dramatically decrease the effectiveness of the control system and it still provides reasonably good results.

A comparison of the performance of the autoresonant control based on the phase control algorithm with the conventional frequency control, regime without feedback, was undertaken when the system was excited with predefined frequency. The simulation showed that forced oscillations cannot control the level of vibrations at all. When the load was applied, the resonant frequency of the system was changed and, as it was excited with a different frequency, the oscillations were gradually damped.

5. Conclusions

Autoresonant control is the method of control of ultrasonically assisted machining, providing monitoring of ultrasonic vibrations in the most efficient way. It allows keeping the nonlinear resonant mode of vibrations in ill-defined and time changing conditions.

To a great extent, the efficiency of control depends on the feedback design, which in its turn relies on the sensor. Three control strategies based on signals from different sensors have been investigated and compared, these are: mechanical feedback (displacement control) and two cases of electrical feedback (current control and power control).

The completed investigation revealed that the control system based on mechanical feedback provides the most efficient means of control. Advantages of mechanical feedback are linked to the location of the sensor. In the case of mechanical feedback, the sensor is placed near the cutting zone and provides the most reliable information about the dynamics of the machining process.

Electrical feedback is based on the sensor measuring the electrical characteristics of the piezoelectric transducer, which reflects the real vibrations of the ultrasonic system in an indirect way. The piezoelectric transducer is distant from the cutting zone and its electrical characteristics (current and power) are much less subject to the influence of the cutting process than are the mechanical characteristics. This explains the inefficiency of the control system with electrical feedback.

The limited possibilities of electrical feedback can be improved by improving the correlation with the machining process. This can be done, for example, by introduction of an additional sensor measuring the load applied to the ultrasonic transducer. This would help to monitor the dynamics of the machining process and would improve the reliability of the electrical feedback. Another area of development is the coordination of the resonances of the electrical system, comprising the piezoelectric transducer, which is substantially capacitive, and matchbox (the interfacing device matching the output of an amplifier with the input of the piezoelectric transducer), which is mostly inductive, and the mechanical system, representing the concentrator of the ultrasonic transducer. It is suggested that a coincidence of resonances of electrical and mechanical systems will substantially improve the consistency of electrical feedback.

References

[1] A.I. Markov, *Ultrasonic Machining of Intractable Materials*, Iliffe Books Ltd., London, 1966.
[2] J. Kumabe, *Vibration Cutting*, Jikkyou Publishing Co., Tokyo, 1979 (in Japanese).
[3] V.I. Babitsky, *Theory of Vibro-Impact Systems and Applications*, Springer, Berlin, 1998.
[4] V.I. Babitsky, A.N. Kalashnikov, F.V. Molodtsov, Autoresonant control of ultrasonically assisted cutting, *Mechatronics* 14 (1) (2004) 91–114.
[5] V.K. Astashev, V.I. Babitsky, *Ultrasonic Processes and Machines. Dynamics, Control and Applications*, Springer, Berlin, 2007.
[6] V.I. Babitsky, Autoresonant mechatronic systems, *Mechatronics* 5 (1995) 483–495.
[7] T. Suzuki, S. Kaneko, K. Takeda, A design of constant velocity feedback power oscillator, Ultrasonics Second World Congress, Yokohama, Japan, 1997, pp. 154–155.
[8] N.N. Abboud, et al., Finite element modelling of ultrasonic transducers, Proceedings—SPIE the International Society for Optical Engineering, issue 3341, 1998, pp. 19–42.
[9] Morgan Electroceramics, Piezoelectric ceramics: Properties & Applications, 〈http://www.morganelectroceramics.com/pzbook.html#pdf9〉.
[10] V.K. Astashev, A.R. Sakayan, Experimental investigation of the dynamics of the vibrating system of an ultrasonic lathe, *Mashinovedenie* 4 (3–7) (1967) (in Russian).
[11] I.J. Sokolov, V.I. Babitsky, Phase control of self-sustained vibration, *Journal of Sound and Vibration* 248 (4) (2001) 725–744.